Fully-disposable multilayered phononic crystal liquid sensor with symmetry reduction and a resonant cavity

S. Villa-Arango [a,b,*], R. Torres [a], P.A. Kyriacou [b], R. Lucklum [c]

[a] Biomedical Engineering Research Group EIA – CES (GIBEC), EIA University, Envigado 055420, Colombia
[b] Research Centre for Biomedical Engineering (RCBE), City University London, London EC1V 0HB, UK
[c] Institute of Micro and Sensor Systems (IMOS), Otto-von-Guericke-University, Magdeburg D39106, Germany

Keywords:
Phononic crystals
Cavity resonance
Symmetry reduction
Defect mode
Biomedical sensor
Point of care technologies
Acoustic wave sensor

A B S T R A C T

Phononic crystals are artificial structures with unique capabilities to control the transmission of acoustic waves. These novel periodic composite structures bring new possibilities for developing a fundamentally new sensor principle that combines features of both ultrasonic and resonant sensors. This paper reports the design, fabrication and evaluation of a phononic crystal sensor for biomedical applications, especially for its implementation in point of care testing technologies. The key feature of the sensor system is a fully-disposable multi-layered phononic crystal liquid sensor element with symmetry reduction and a resonant cavity. The phononic crystal structure consists of eleven layers with high acoustic impedance mismatch. A defect mode was utilized in order to generate a well-defined transmission peak inside the bandgap that can be used as a measure. The design of the structures has been optimized with simulations using a transmission line model. Experimental realizations were performed to evaluate the frequency response of the designed sensor using different liquid analytes. The frequency of the characteristic transmission peaks showed to be dependent on the properties of the analytes used in the experiments. Multi-layered phononic crystal sensors can be used in applications, like point of care testing, where the on-line measurement of small liquid samples is required.

1. Introduction

Phononic crystals, PnC, are composite materials possessing a periodic and spatial modulation of their acoustic properties, allowing them to have control over a selective transmission of mechanical elastic waves in solids, and pressure waves in liquids. Like their optical counterparts, photonic crystals, these crystals enable the configuration of their working frequency by fine-tuning the geometry and dimensions of the structure. Some authors have even worked in frequency control strategies by means of using materials with very interesting magnetoelastic and electrorheological properties [1–4].

The graphical representation of a phononic crystal shown in Fig. 1(a) is composed of a homogeneous matrix and a number of scattering centers with an acoustic impedance different to the matrix to facilitate the dispersion of waves. The most obvious feature of PnCs are frequency bands in which the crystal behaves like a mirror reflecting waves of all directions of incidence, Fig. 1(b). These frequency bands are called bandgaps or forbidden bands and their design allows controlling the selective transmission of waves in phononic crystals [1,2,5].

Phononic crystals can be classified by their topology in two categories: cermet or network. Crystals with a cermet topology are also called acoustic phononic crystals and are composed of a liquid matrix and embedded solid scatterers with high density. On the other hand, crystals with a network topology, or elastic phononic crystals, have a solid matrix and low-density scattering units [6,7].

The design of PnC can also be conceived in structures with a reduction in their dimensionality using an approximation to 1-D. These structures are not formed by a matrix with embedded scattering units, but by a series of consecutive thin layers with large acoustic impedance mismatch and with lateral dimensions much larger than their thickness. The layers are organized in a periodic way that enables a spatial modulation of the acoustic properties throughout the structure and facilitates the selective reflection of acoustic and elastic waves and therefore the generation of bandgaps. A graphical representation of a 1-D phononic crystal can be observed in Fig. 2 [8].

* Corresponding author at: Biomedical Engineering Research Group EIA – CES (GIBEC), EIA University, Envigado 055420, Colombia.
E-mail address: simon.villa@eia.edu.co (S. Villa-Arango).

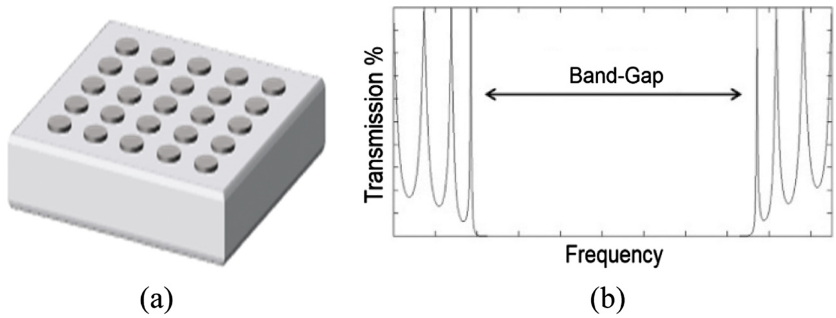

Fig. 1. Graphical representation of a phononic crystal composed of a homogeneous matrix and a series of cylindrical inclusions arranged in a square matrix (a) and its respective frequency response displaying an ideal bandgap (b).

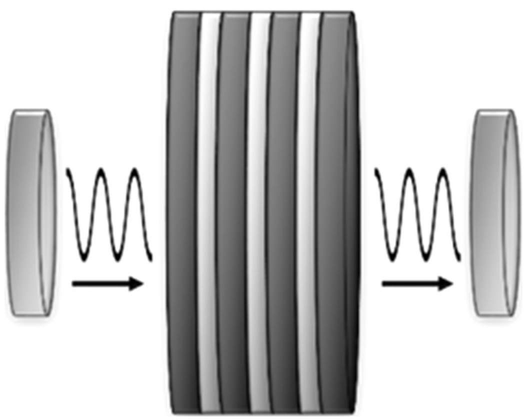

Fig. 2. Graphical representation of a 1-D phononic crystal composed of a series of consecutive thin layers with high acoustic impedance mismatch. On the sides are two ultrasonic transducers, represented by gray discs, generating and receiving the signal used to characterize its frequency response.

The design of bandgaps in 1-D phononic crystals is performed by adapting the thickness of each layer so that the maximum reflection, or minimum transmission, is located in the wanted frequency range. The bandwidth and depth of the generated bandgap will depend on the ratio of acoustic impedances between consecutive layers. The larger it is, the larger the scattering effect of the structure, generating a wider frequency range with large acoustic rejection over which acoustic waves are not transmitted [8].

There are numerous methods for simulating the frequency response of phononic crystals including the one-dimensional transmission line model (TLM), the eigenmodes matching theory (EMMT), the layer multi-scattering theory (LMST), the plane wave expansion method (PWE), the finite element method (FEM) and the finite difference time domain (FDTD) among others. The transmission line model is especially used when calculating multi-layered structures, giving adequate results and reducing the amount of computation power and time to realize the simulations. It has been previously used to calculate the transmission spectrum of phononic crystals with good results [9–14].

The propagation of acoustic waves in phononic crystals is described in the TLM using an analogy to electrical waves, see Table 1. This model considers homogeneous, isotropic, uniform layers with minimum effect of the lateral dimensions on the propagation of acoustic waves. The effective acoustic impedance contains the relevant characteristic acoustic parameters and layer thickness, e, of each layer composing the PnC. The transmission and reflection coefficients are calculated using an overall effective acoustic impedance of the PnC, Z_L. It is important to notice that the effective acoustic impedance is frequency dependent and is different from the characteristic impedance of the material, Z_c, which is equal to the density, ρ, multiplied by the speed of sound of the material, c. The concept considers the reflection and transmission of waves in layer interfaces and also inside each layer [9,13]. The effective acoustic impedance of layer i can be calculated using Eq. (1).

$$Z_{L(i+1)} = Z_{c(i)} \frac{Z_{L(i)} + jZ_{c(i)} tan(2\pi fe/c)}{Z_{c(i)} + jZ_{L(i)} tan(2\pi fe/c)} \quad (1)$$

Table 1
Equivalences between the electrical and acoustic parameters.

Mechanical tension	T ⇒ U	Electrical voltage
Particle velocity	v ⇒ I	Electrical current
Acoustic impedance	Z = T/v ⇒ Z = U/I	Electrical impedance

The selective control of elastic and acoustic waves using phononic crystals more and more attracts the attention of the scientific community around the world to apply the novel resonant structures in diverse applications, among which are: wave guiding, acoustic insulation, acoustic cloaking, heat phonon transmission, multiplexing and demultiplexing of waves, and more recently, sensing [15–24].

Both surface acoustic waves, SAW, and bulk acoustic waves, BAW, have been studied in the development of phononic crystal sensors. SAW resonators have working frequencies up to GHz frequencies and the lattice constant goes down to micrometers and even micrometers [22,25,26]. Some authors have even explored the possibility of designing dual phononic-photonic crystals, these structures are called phoxonic crystals and they are used to study the simultaneous control of the propagation of acoustic and electromagnetic waves [23,27–29]. BAW sensors typically work in the range of MHz and can use both pressure and/or shear waves. The lattice constant of respective PnC sensors is in the order of 100's of micrometers to a few millimeters. Those dimensions agree with common MEMS technology and enable the implementation of microfluidic systems and solid/liquid sub-structures [16–21,24].

The concept of the phononic crystal sensors for liquids is based on the introduction of defect modes that appear as relevant transmission features inside bandgaps and are visible in the transmission spectrum of the phononic crystal. Defect modes can be realized by point, line or plane defects that are introduced in an otherwise regular periodic structure. Liquid samples that are going to be analyzed, shortly analytes, become part of the phononic crystal. Therefore, any variation in the acoustic properties of the analyte causes changes in the frequency of the defect modes. Phononic crystal liquid sensors basically measure the longitudinal speed of sound of small liquid samples. However, the speed of sound of liquids and liquid mixtures is finally defined by molar mass, molar volume and adiabatic compressibility of the components as well as the molar ratio and is directly linked to intermolecular interactions in complex mixtures. Therefore, phononic crystals can be classified as chemical sensors [14].

One big difference between phononic crystals and other resonant sensors, like the quartz crystal microbalance, QCM, is that PnC allows to perform an evaluation of the volumetric properties of liquid samples and not of properties of the liquid at an interface. PnC sensors combine the characteristics of resonant sensors and ultrasonic sensors by using the propagation of acoustic waves through liquids and measuring changes in the frequency response of the system to determine its properties [30,31].

This paper reports the design, manufacture, and evaluation of a fully-disposable multi-layered phononic crystal liquid sensor with symmetry reduction and a resonant cavity that can be used in applications that require the measurement of small liquid samples in the field. In order to realize the measurement of the frequency spectrum of the system, a characterization system for measuring frequency changes of resonant structures like PnC was used [32]

The designed sensor contains a resonant cavity filled with the analyte that generates a defect mode that appears as a maximum of transmission located inside the bandgap. Increasing the quality factor of this transmission peak is essential for the precision of the measurement. Our structure of this multi-layered phononic crystal is made of glass and PLA and can be discarded after the test, thus avoiding disinfection methods and improving the usability of this system in field applications with biological substances like in point of care testing.

2. Materials and methods

The sensing system presented in this paper has 3 main components: the multi-layered PnC sensor, a pair of ultrasonic transducers and an electronic characterization system. The multi-layered PnC sensor was designed for the measurement of liquid samples with acoustic properties similar to water, i.e., with a longitudinal component of the speed of sound close to 1500 m/s and a value of its mass density around 1000 kg/m^3. Knowing that the analyte becomes part of the phononic crystal structure, special care must be taken when selecting the materials composing the layers that are in contact with the analyte. Beside (bio) chemical issues like biocompatibility, an impedance mismatch is required for allowing the generation of bandgaps with adequate bandwidth and depth for sensing applications. We have selected glass as the material to form the layers that are facing the analyte. The selected glass has an acoustic impedance of 13.77 MRayls, resulting in an acoustic impedance ratio of 9.18 with the analyte.

The phononic crystal sensor structure was designed using 11 layers: 4 glass layers, 5 analyte layers and 2 PZT outer layers, the latter corresponding to the ultrasonic transducers. A schematic representation of the layer arrangement of the PnC structure can be seen in Fig. 3. The lateral dimensions of the layers are much larger than their thickness and the multilayered PnC sensor can be approximated to a 1-D structure.

To give support to the multilayer structure and realize alignment, a container made of polylactic acid, PLA, was designed. PLA is a low-cost thermoplastic polyester composed of lactic acid molecules that can be obtained from renewable resources like corn and sugarcane making it biodegradable and ideal to form part of the disposable element of the sensor. For manufacturing the PLA container, a fused filament fabrication, FFF, 3-D printer with a 0.4 mm extruder head and a 0.08 mm layer resolution was used.

The selected ultrasonic transducers have a central frequency of 1.1 MHz and a large bandwidth, therefore, the calculation of the dimensions of the layers of the PnC sensor was performed using as central frequency or working frequency being the same frequency as the ultrasonic transducers. The selected transducers predominantly generate longitudinal waves in order to favor the transmission of waves through the liquid layers of the structure. The ultrasonic transducers are in direct contact with the outer liquid layers of the phononic crystal, thus, eliminating the need of using additional coupling media.

The dimensions of the glass and analyte layers were calculated following the equation of minimum transmission through, or maximum reflection at the thin layers. In order to obtain a minimum of transmission at a specific frequency, the layer thickness, d_R, must be equal to an uneven multiple of the wavelength, λ, divided by four, Eq. (2) [33,34].

$$d_R = (2n - 1)\lambda/4 \tag{2}$$

Knowing that the wavelength is equal to the speed of sound of the material divided by the frequency and that the speed of sound of the glass layers is 5100 m/s and of the analyte layers is 1500 m/s, a layer thickness of 1.159 mm was selected for the glass layers, Eq. (3), and of 1.022 mm for the analyte layers, Eq. (4) [33,34].

$$d_g = (2n - 1)5100\ (\mathrm{m/s})/4(1.1\ (\mathrm{MHz})) = (1)1.159\ \mathrm{mm} \tag{3}$$

$$d_a = (2n - 1)1500\ (\mathrm{m/s})/4(1.1\ (\mathrm{MHz})) = (3)341\ \mu\mathrm{m} \tag{4}$$

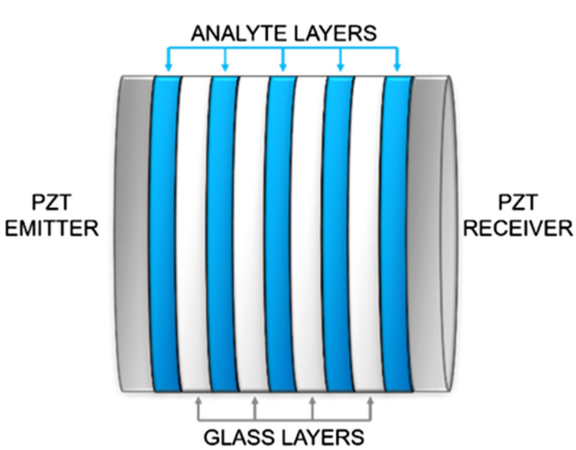

Fig. 3. Schematic representation of the layer arrangement of the PnC structure.

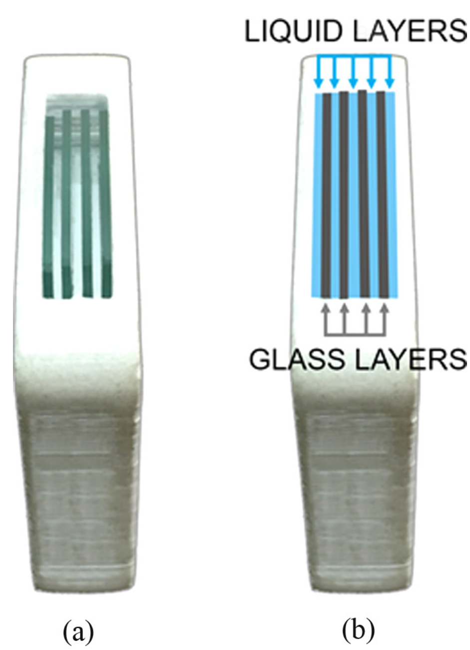

Fig. 4. First phononic crystal structure fabricated using the 3-D printer and glass.

After calculating the values of the dimensions of the layers to have a bandgap with a central frequency around 1.1 MHz, the next step was to conduct a series of simulations to observe the behavior of a phononic crystal with these characteristics. The simulations were performed using the 1-D transmission line model and distilled water and ethanol from ProtoKimica (Medellin, Colombia) were used as analytes to evaluate its frequency dependence of characteristic transmission features. In addition to the theoretical realizations, the PnC structure was fabricated using the 3-D printer and a series of experimental tests were conducted to confirm the theoretical results. The fabricated structure is shown in Fig. 4. Microscope slides from Glass Lab (San Bernardo, Chile) where used to form the glass layers. The thickness of these borosilicate glass slides is 1.1 mm making the ideal for their use in the PnC structure.

The first structure designed has a regular periodicity. Dimensions have been chosen to form a bandgap around 1.1 MHz. In order to be able to achieve a well-defined transmission feature in the frequency spectrum that can be characterized and used as a measure in a sensing system for biomedical applications, symmetry reduction by means of introducing a defect has been implemented in the phononic crystal. It has been realized by changing the dimensions of the central liquid layer. The equation of maximum transmission through thin layers was used to calculate the optimal value, Eq. (5). 2.045 mm was obtained for the layer thickness of the defect layer, twice the original value, Eq. (6). Note that we have found that there is a higher chance of obtaining good experimental results when using the same value of n for all the layers.

$$d_T = n\lambda/2 \tag{5}$$

$$d_T = 1500\ (\mathrm{m/s})/2(1.1\ (\mathrm{MHz})) = (3)682\ \mu\mathrm{m} \tag{6}$$

Just as in the previous structure, theoretical investigations were performed in order to evaluate the behavior in frequency of the designed PnC sensor. After the calculations, the PnC multilayered sensor was manufactured using the 3-D fabrication method and was evaluated experimentally using binary mixtures; ethanol solutions in distilled water at low concentrations were used to estimate the sensor sensitivity in frequency. The fabricated structure is shown in Fig. 5.

A portable electronic characterization system that allows carrying out accurate measurements of frequency changes in resonant structures and phononic crystals using a pair of high-frequency ultrasonic transducers was used. The system operates on a double sideband modulation with suppressed carrier and a special demodulation process using filters that allow acquiring gain and phase values of the system in a predetermined frequency range [32].

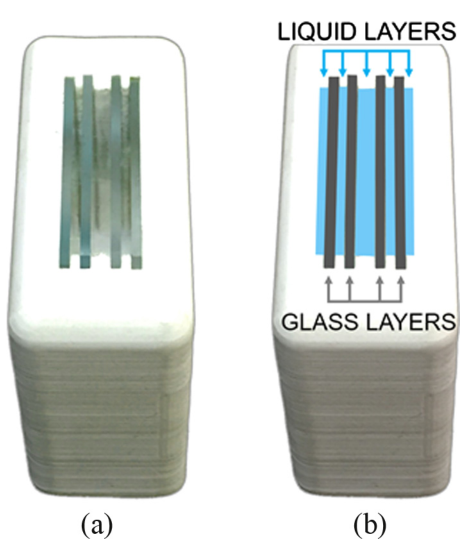

Fig. 5. Second phononic crystal structure designed with a defect mode and fabricated using the 3-D printer and glass. The central liquid layer has a different thickness than the other liquid layers in order to generate a transmission band inside the bandgap.

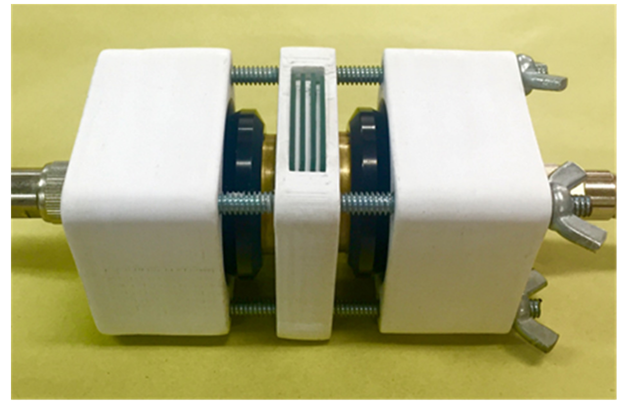

Fig. 6. Experimental arrangement containing the designed structure, the transducers, and the electronic characterization system.

Table 2
Properties of the Materials used for the simulations.

Material	c (m/s)	p (kg/m^3)	Zc (MRayls)
Glass	5100	2700	13.5
PZT	3055	7500	22.91
Water	1493	998	1.49
Ethanol	1156	790	9.13

The electronic system was set to acquire 1300 points going from 0.5 MHz to 1.8 MHz. The frequency steps were set to 100 Hz. The PnC sensor was thoroughly rinsed and dried before introducing a new sample. The alcohol samples were carefully handled in order to avoid evaporation. The temperature of the system was kept constant using room temperature control. The experimental arrangement used for the tests is depicted in Fig. 6 and is composed of the two ultrasonic transducers, the phononic crystal and a 3-D printed holding structure to give support to the transducers. The properties of the analytes and materials used for the simulations of both phononic crystal structures are summarized in Table 2. The material properties were calculated using data from [35,36].

3. Results and discussion

Fig. 7 shows the simulation results of the first structure using the 1-D transmission line model. Water (a) and ethanol (b) were used as analytes to evaluate its frequency response. The computational results show a typical behavior of a phononic crystal with both analytes producing well-defined bandgaps with similar bandwidth. The central frequency of the bandgap produced using water is located around 1.1 MHz and the ones produced using ethanol are located around 850 kHz and 1.45 MHz. The difference between the frequency response of water and ethanol arises from the differences in the respective speed of sound of the analytes.

Fig. 8(a) shows the simulation results of the second structure using the 1-D transmission line model. This time, distilled water was used as analyte to evaluate its frequency response. The computational results show that the inclusion of a defect mode has generated the appearance of a transmission peak in the middle of the bandgap. Fig. 8(b) shows a close-up of the central transmission peak which has a good amplitude and a high-quality factor. The surrounding bandgap isolates it from possible noise sources generating suitable boundary conditions for sensing applications.

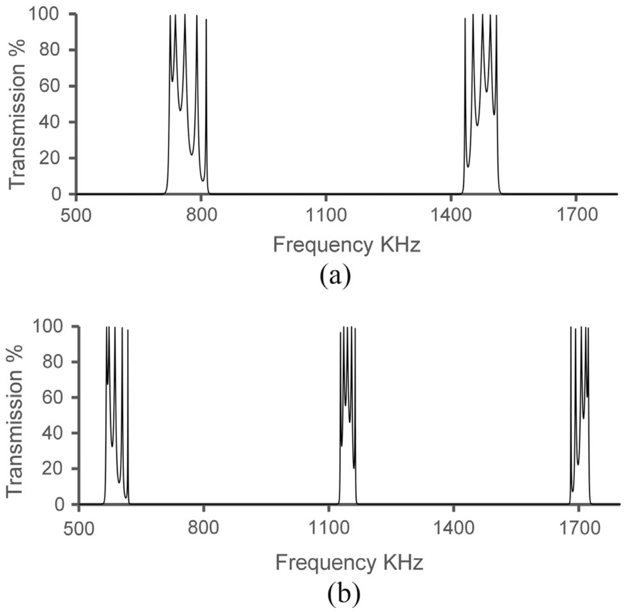

Fig. 7. Simulation results of the first structure using distilled water (a) and ethanol (b) as analytes.

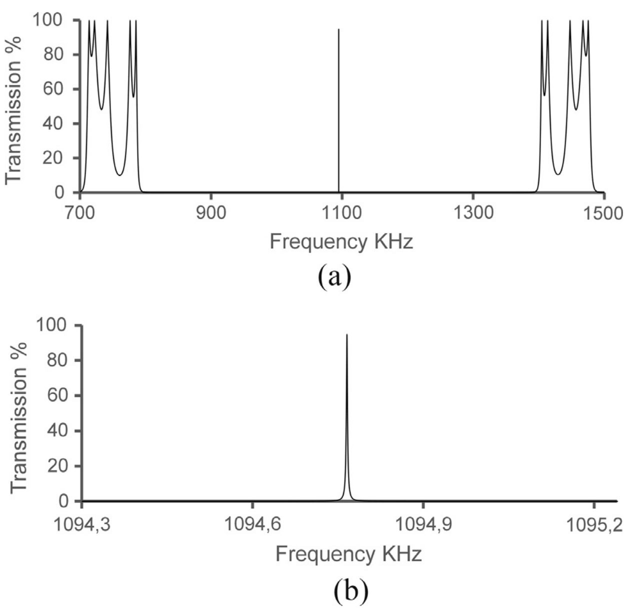

Fig. 8. Simulation results of the second structure using distilled water as analyte (a) along with a close-up of the main transmission peak around 1.1 MHz (b).

After performing the simulations, the designed structures were fabricated and evaluated using the double sideband electronic characterization system previously described [32].

First, the performance of the phononic crystal structure designed without using defect modes was experimentally evaluated. Fig. 9, shows the experimental results of the first structure using water (a) and ethanol (b) as analytes.

The experimental results using the first structure show the characteristic behavior in frequency of phononic crystals, which is a selective transmission of waves with bandgaps located in different frequency ranges depending on the properties of the constituent materials and dimensions of the layers. Ethanol has a lower speed of sound than distilled water, therefore, the central frequency of the bandgaps generated by the PnC structure is lower when ethanol is used as analyte.

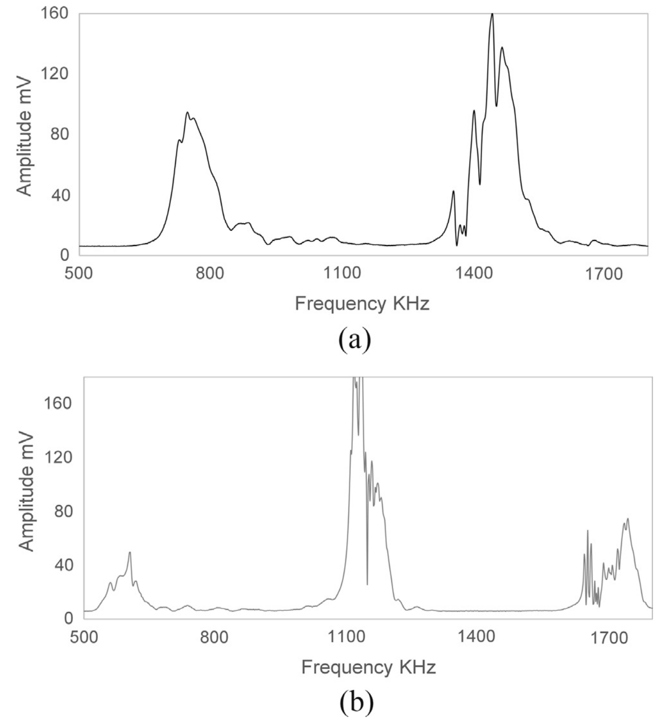

Fig. 9. Experimental results of the first structure using distilled water (a) and ethanol (b) as analytes.

The experimental results are in accordance to the simulations, with bandgaps located at the same frequencies having similar bandwidths. Differences between simulation and experiments must be addressed mainly to the finite lateral size of the plates and liquid cavities.

Following the same protocol as in the 1-D simulations, binary mixtures of ethanol in water with a concentration of 0.02% and 0.5% in volume fraction were used to experimentally evaluate the performance of the second structure, Fig. 10.

The experimental results obtained with the second structure show a bandgap between 0.8 MHz and 1.4 MHz with a transmission peak located close to 1.1 MHz, as expected from simulations. The transmission peak inside the band gap is easy to detect. It is significantly elevated above the noise floor and well separated from other transmission signals. Again, the latter are not present in the simulations for the above reasons. Small material defects or misalignment can also cause the experimental results to deviate from the theoretical ones.

Fig. 11 shows a close-up on the central peak of the experimental results of the second structure and compares the frequency response of both analytes. The variations in the concentration of

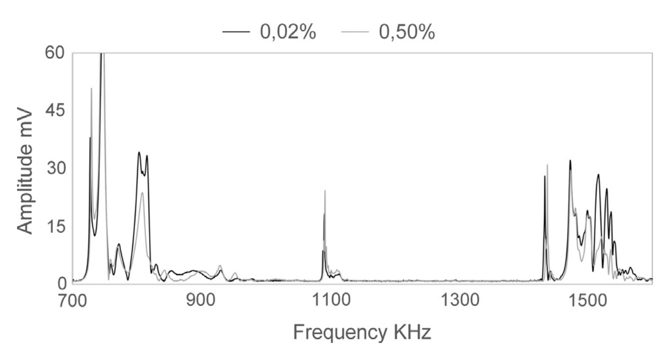

Fig. 10. Experimental results of the second structure using ethanol solutions in water with a concentration of 0.02% and 0.5% in volume fraction.

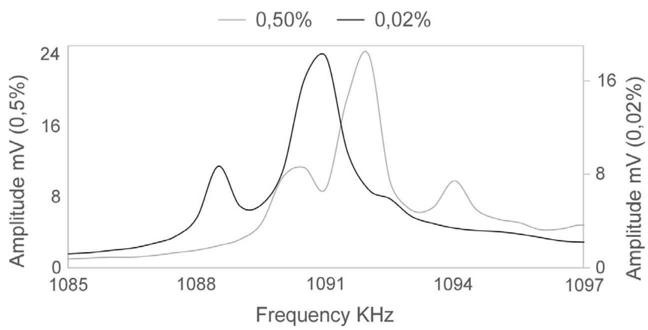

Fig. 11. Comparison of the experimental results of the second structure using ethanol solutions in water with a concentration of 0.02% (black) and a concentration of 0.5% (gray) in volume fraction.

the analyte, here ethanol in water, correspond to a shift in frequency of the designed transmission feature. The importance of having a sharp transmission peak to be able to differentiate this change becomes obvious as well. Currently, the central transmission peak has a good quality factor, however, in order to facilitate its use in sensing applications at very low concentration, improvements in this value are required. The simulations show that there is enough space for improvements and ongoing engineering activities deal with justification of the experimental setup and manufacturing to minimize unwanted deviations from the theoretical assumption like parallelism of the building layers.

The main transmission peak was displaced to higher frequencies when the amount of ethanol in water increased, despite the fact that ethanol has a lower speed of sound than distilled water. This result was expected due to the behavior of the speed of sound of ethanol – water mixtures. At low concentrations, it starts to increase until it reaches a peak when the mole fraction is equal to 0.133 and then starts to decrease [35].

4. Conclusions

A multi-layered phononic crystal liquid sensor utilizing defect modes to generate a well-defined transmission peak inside the bandgap of the regular 1-D Phononic crystal for measuring variations in the concentration of analytes in small liquid samples was developed.

Design and material selection consider the usage of the introduced sensor system as sensing modality in biomedical applications including point of care testing where disposable sensor elements are favored.

This ultrasonic technology measures mechanical properties of the liquid samples instead of optical or electrical properties like most of the current sensor technologies. In consequence, the speed of sound must be related to the (bio) chemical values of interest as the concentration of some substance in a liquid mixture or solution.

References

[1] M. Sigalas, E. Economou, Elastic and acoustic wave band structure, J. Sound Vib. 158 (1992) 377–382, http://dx.doi.org/10.1016/0022-460x(92)90059-7.
[2] M. Kushwaha, P. Halevi, L. Dobrzynski, B. Djafari-Rouhani, Acoustic band structure of periodic elastic composites, Phys. Rev. Lett. 71 (1993) 2022–2025, http://dx.doi.org/10.1103/physrevlett.71.2022.
[3] J. Robillard, O. Matar, J. Vasseur, P. Deymier, M. Stippinger, A. Hladky-Hennion, Y. Pennec, B. Djafari-Rouhani, Tunable magnetoelastic phononic crystals, Appl. Phys. Lett. 95 (2009) 124104, http://dx.doi.org/10.1063/1.3236537.
[4] J. Yeh, Control analysis of the tunable phononic crystal with electrorheological material, Physica B 400 (2007) 137–144, http://dx.doi.org/10.1016/j.physb.2007.06.030.
[5] J. Vasseur, P. Deymier, G. Frantziskonis, G. Hong, B. Djafari-Rouhani, L. Dobrzynski, Experimental evidence for the existence of absolute acoustic band gaps in two-dimensional periodic composite media, J. Phys.: Condens. Matter 10 (1998) 6051–6064, http://dx.doi.org/10.1088/0953-8984/10/27/006.
[6] E. Economou, M. Sigalas, Classical wave propagation in periodic structures: cermet versus network topology, Phys. Rev. B 48 (1993) 13434–13438, http://dx.doi.org/10.1103/physrevb.48.13434.
[7] N. Aravantinos-Zafiris, M. Sigalas, M. Kafesaki, E. Economou, Phononic crystals and elastodynamics: some relevant points, AIP Adv. 4 (2014) 124–203, http://dx.doi.org/10.1063/1.4904406.
[8] E. Elboudouti, Acoustic waves in solid and fluid layered materials, Surf. Sci. Rep. 64 (2009) 471–594, http://dx.doi.org/10.1016/j.surfrep.2009.07.005.
[9] R. Lucklum, C. Behling, R. Cernosek, S. Martin, Determination of complex shear modulus with thickness shear mode resonators, J. Phys. D Appl. Phys. 30 (1997) 346–356, http://dx.doi.org/10.1088/0022-3727/30/3/006.
[10] Z. Hou, B. Assouar, Transmission property of the one-dimensional phononic crystal thin plate by the eigenmode matching theory, J. Phys. D Appl. Phys. 41 (2008) 095103, http://dx.doi.org/10.1088/0022-3727/41/9/095103.
[11] C. Qiu, Z. Liu, J. Mei, M. Ke, The layer multiple-scattering method for calculating transmission coefficients of 2D phononic crystals, Solid State Commun. 134 (2005) 765–770, http://dx.doi.org/10.1016/j.ssc.2005.02.034.
[12] Y. Tanaka, Y. Tomoyasu, S. Tamura, Band structure of acoustic waves in phononic lattices: two-dimensional composites with large acoustic mismatch, Phys. Rev. B 62 (2000) 7387–7392, http://dx.doi.org/10.1103/physrevb.62.7387.
[13] R. Lucklum, D. Soares, K. Kanazawa, Models for resonant sensors, in: A. Arnau (Ed.), Piezoelectric Transducers and Applications, Springer, 2008, pp. 63–96.
[14] R. Lucklum, J. Li, Phononic crystals for liquid sensor applications, Meas. Sci. Technol. 20 (2009) 124014, http://dx.doi.org/10.1088/0957-0233/20/12/124014.
[15] Y. Pennec, J. Vasseur, B. Djafari-Rouhani, L. Dobrzyński, P. Deymier, Two-dimensional phononic crystals: examples and applications, Surf. Sci. Rep. 65 (2010) 229–291, http://dx.doi.org/10.1016/j.surfrep.2010.08.002.
[16] R. Lucklum, J. Li, M. Zubtsov, 1D and 2D phononic crystal sensors, Proc. Eng. 5 (2010) 436–439, http://dx.doi.org/10.1016/j.proeng.2010.09.140.
[17] M. Ke, M. Zubtsov, R. Lucklum, Sub-wavelength phononic crystal liquid sensor, J. Appl. Phys. 110 (2011) 026101, http://dx.doi.org/10.1063/1.3610391.
[18] M. Zubtsov, R. Lucklum, M. Ke, A. Oseev, R. Grundmann, B. Henning, U. Hempel, 2D phononic crystal sensor with normal incidence of sound, Sens. Actuat., A 186 (2012) 118–124, http://dx.doi.org/10.1016/j.sna.2012.03.017.
[19] R. Lucklum, S. Villa, M. Zubtsov, Cavity resonance biomedical sensor, in: IMECE2014-38222: ASME 2014 International Mechanical Engineering Congress and Exposition, Montreal, Quebec, Canada, 2014.
[20] R. Lucklum, S. Villa, M. Zubtsov, R. Grundmann, Phononic cystal sensor for medical applications, in: IEEE SENSORS 2014, Valencia, Spain, Proc., 2014, pp. 903–906.
[21] S. Villa-Arango, R. Torres Villa, P. Kyriacou, R. Lucklum, Cavity resonance sensor with disposable analyte container for point of care testing, IEEE Sensors J. 16 (2016) 6727–6732, http://dx.doi.org/10.1109/jsen.2016.2584240.
[22] R. Olsson III, I. El-Kady, Microfabricated phononic crystal devices and applications, Meas. Sci. Technol. 20 (2008) 012002, http://dx.doi.org/10.1088/0957-0233/20/1/012002.
[23] S. Amoudache, Y. Pennec, B. Djafari Rouhani, A. Khater, R. Lucklum, R. Tigrine, Simultaneous sensing of light and sound velocities of fluids in a two-dimensional phoXonic crystal with defects, J. Appl. Phys. 115 (13) (2014) 134503.
[24] A. Salman, O. Kaya, A. Cicek, Determination of concentration of ethanol in water by a linear waveguide in a 2-dimensional phononic crystal slab, Sens. Actuat., A 208 (2014) 50–55.
[25] D. Nardi, F. Banfi, C. Giannetti, B. Revaz, G. Ferrini, F. Parmigiani, Pseudosurface acoustic waves in hypersonic surface phononic crystals, Phys. Rev. B 80 (10) (2009).
[26] C. Hou, V. Zhang, H. Lim, S. Ng, M. Kuok, J. Deng, S. Wang, Band structures of surface acoustic waves in nanostructured phononic crystals with defects, Appl. Phys. Lett. 105 (24) (2014) 243104.
[27] R. Lucklum, M. Zubtsov, A. Oseev, Phoxonic crystals—a new platform for chemical and biochemical sensors, Anal. Bioanal. Chem. 405 (2013) 6497–6509, http://dx.doi.org/10.1007/s00216-013-7093-9.
[28] T. Ma, Y. Wang, C. Zhang, X. Su, Theoretical research on a two-dimensional phoxonic crystal liquid sensor by utilizing surface optical and acoustic waves, Sens. Actuat., A 242 (2016) 123–131, http://dx.doi.org/10.1016/j.sna.2016.03.003.
[29] B. Djafari-Rouhani, S. El-Jallal, Y. Pennec, Phoxonic crystals and cavity optomechanics, C. R. Phys. 17 (5) (2016) 555–564.
[30] A. Arnau, Piezoelectric Transducers and Applications, second ed., Springer, Berlin, 2008, ISBN: 978-3-540-77507-22.
[31] Y. Montagut, J. Garcia, Y. Jimenez, C. March, A. Montoya, A. Arnau, QCM technology in biosensors, Biosens. - Emerg. Mater. Appl. (2011), http://dx.doi.org/10.5772/17991.
[32] S. Villa, R. Torres, R. Lucklum, Electronic characterisation system for measuring frequency changes in phononic crystals, Electron. Lett. 51 (2015) 545–546, http://dx.doi.org/10.1049/el.2014.4151.
[33] H. Pain, The Physics of Vibrations and Waves, John Wiley, Chichester, 2005.
[34] R. Millner, Wissensspeicher Ultraschalltechnik, Fachbuchverlag, Leipzig, 1987.
[35] R. Kuhnkies, W. Schaaffs, Untersuchungen an adiabatisch und isotherm aufgenommenen Schallkennlinien binärer Mischungen, Acustica 13 (1963) 407.
[36] D.R. Lide, CRC Handbook of Chemistry and Physics, 84th ed., CRC Press, Boca Raton, 2004.